Estrogen promotes Leydig cell engulfment by macrophages in male infertility

Wanpeng Yu, … , Ituro Inoue, Xiangdong Li

Research Article **Endocrinology**

Male infertility accounts for almost half of infertility cases worldwide. A subset of infertile men exhibit reduced testosterone and enhanced levels of estradiol (E2), though it is unclear how increased E2 promotes deterioration of male fertility. Here, we utilized a transgenic mouse strain that overexpresses human *CYP19*, which encodes aromatase (AROM+ mice), and mice with knockout of *Esr1*, encoding estrogen receptor α (ERαKO mice), to analyze interactions between viable Leydig cells (LCs) and testicular macrophages that may lead to male infertility. In AROM+ males, enhanced E2 promoted LC hyperplasia and macrophage activation via ERα signaling. E2 stimulated LCs to produce growth arrest–specific 6 (GAS6), which mediates phagocytosis of apoptotic cells by bridging cells with surface exposed phosphatidylserine (PS) to macrophage receptors, including the tyrosine kinases TYRO3, AXL, and MER. Overproduction of E2 increased apoptosis-independent extrusion of PS on LCs, which in turn promoted engulfment by E2/ERα-activated macrophages that was mediated by AXL-GAS6-PS interaction. We further confirmed E2-dependant engulfment of LCs by real-time 3D imaging. Furthermore, evaluation of molecular markers in the testes of patients with nonobstructive azoospermia (NOA) revealed enhanced expression of CYP19, GAS6, and AXL, which suggests that the AROM+ mouse model reflects human infertility. Together, these results suggest that GAS6 has a potential as a clinical biomarker and therapeutic target for male infertility.

Find the latest version:

Estrogen promotes Leydig cell engulfment by macrophages in male infertility

Wanpeng Yu,[1] Han Zheng,[1] Wei Lin,[1] Astushi Tajima,[2] Yong Zhang,[1] Xiaoyan Zhang,[3] Hongwen Zhang,[4] Jihua Wu,[4] Daishu Han,[3] Nafis A. Rahman,[5] Kenneth S. Korach,[6] George Fu Gao,[7] Ituro Inoue,[2] and Xiangdong Li[1]

[1]State Key Laboratory of Agrobiotechnology, College of Biological Sciences, China Agricultural University, Beijing, People's Republic of China. [2]Division of Human Genetics, National Institute of Genetics, Shizuoka, Japan. [3]Department of Cell Biology, Institute of Basic Medical Sciences, Chinese Academy of Medical Sciences, School of Basic Medicine, Peking Union Medical College, Beijing, People's Republic of China. [4]Department of General Surgery, 306th Hospital of PLA, Beijing, People's Republic of China. [5]Department of Physiology, Institute of Biomedicine, University of Turku, Turku, Finland. [6]Laboratory of Reproductive and Developmental Toxicology–Receptor Biology Group, National Institute of Environmental Health Sciences, NIH, Bethesda, Maryland, USA. [7]CAS Key Laboratory of Pathogenic Microbiology and Immunology, Institute of Microbiology, Chinese Academy of Sciences, Beijing, People's Republic of China.

Male infertility accounts for almost half of infertility cases worldwide. A subset of infertile men exhibit reduced testosterone and enhanced levels of estradiol (E2), though it is unclear how increased E2 promotes deterioration of male fertility. Here, we utilized a transgenic mouse strain that overexpresses human *CYP19*, which encodes aromatase (AROM+ mice), and mice with knockout of *Esr1*, encoding estrogen receptor α (ERαKO mice), to analyze interactions between viable Leydig cells (LCs) and testicular macrophages that may lead to male infertility. In AROM+ males, enhanced E2 promoted LC hyperplasia and macrophage activation via ERα signaling. E2 stimulated LCs to produce growth arrest–specific 6 (GAS6), which mediates phagocytosis of apoptotic cells by bridging cells with surface exposed phosphatidylserine (PS) to macrophage receptors, including the tyrosine kinases TYRO3, AXL, and MER. Overproduction of E2 increased apoptosis-independent extrusion of PS on LCs, which in turn promoted engulfment by E2/ERα-activated macrophages that was mediated by AXL-GAS6-PS interaction. We further confirmed E2-dependant engulfment of LCs by real-time 3D imaging. Furthermore, evaluation of molecular markers in the testes of patients with nonobstructive azoospermia (NOA) revealed enhanced expression of CYP19, GAS6, and AXL, which suggests that the AROM+ mouse model reflects human infertility. Together, these results suggest that GAS6 has a potential as a clinical biomarker and therapeutic target for male infertility.

Introduction

The exposure of phosphatidylserine (PS) on the surface of dead, dying, or aged cells is a universal recognition cue for engulfment by phagocytes (1, 2). Phagocytes interact with PS on target cells with high affinity, either directly through the PS receptor or indirectly through bridging molecules, such as milk-fat globule EGF-8 (MFG-E8) (3) or growth arrest–specific 6 (GAS6) (4). In particular, GAS6 links exposed PS on apoptotic cells to the TYRO3-AXL-MER (TAM) family of receptors on phagocytes, which then activates phagocytosis (5, 6). Expression of PS on the cell surface can occur in a wide variety of disorders, such as Scott's syndrome or thrombocytopenia (7), which may lead to misregulation of phagocytosis.

Male infertility and subinfertility constitute approximately 40%–50% of infertility cases globally (8). Approximately 15% of these cases result from infection or inflammation of the male reproductive tract (i.e., orchitis), and histopathology sections indicate the presence of lymphocytes and macrophages in affected testes (9). Testicular macrophages are increased in a rat model of experimental autoimmune orchitis (EAO) (10). Infiltration of testicular macrophages impairs human testicular function, leading to male infertility (11). However, the signaling pathways that result in macrophage activation remain undefined. A subset of infertile men has significantly lower serum testosterone (T) and higher estradiol (E2) levels (12), indicative of Leydig cell (LC) mal-

function that leads to an increased E2/T ratio. In utero and/or neonatal exposure to excess estrogen in both rodents and humans lead to male genital tract abnormalities, such as cryptorchidism, hypospadia, and impaired spermatogenesis (reviewed in ref. 13). Although the molecular basis for estrogen-induced deterioration of male fertility remains unclear, estrogen receptors (ERs) play a critical role in mediating this process (reviewed in ref. 14). These observations suggest a plausible connection between the estrogen/ERα pathway and the initiation of idiopathic chronic orchitis in a subset of infertile men. However, there are no established molecular mechanisms underlying this phenomenon.

We have previously reported that aging *CYP19*-aromatase transgenic male mice (referred to hereafter as AROM+ mice) present a testicular phenotype of inflammation-associated infertility via the ERα pathway (15). Testicular inflammation is completely absent when AROM+ mice are crossbred with *Esr1*−/− (hereafter ERαKO) mice (16, 17). To examine the molecular mechanisms underlying the effects of E2 or an imbalanced E2/T ratio on infertility, we used AROM+ and ERαKO mice to analyze viable testicular LC engulfment by neighboring macrophages and to determine the long-term consequences of increased E2/T ratio on testicular cell survival in aging AROM+ mice. To assess the human relevance of the mechanistic findings from the AROM+ mouse study, we also analyzed testicular samples and serum E2 and T levels in infertile men presenting with nonobstructive azoospermia (NOA). We also investigated GAS6 as a novel potential clinical biomarker/therapeutic candidate for male infertility caused by an impaired E2/T ratio.
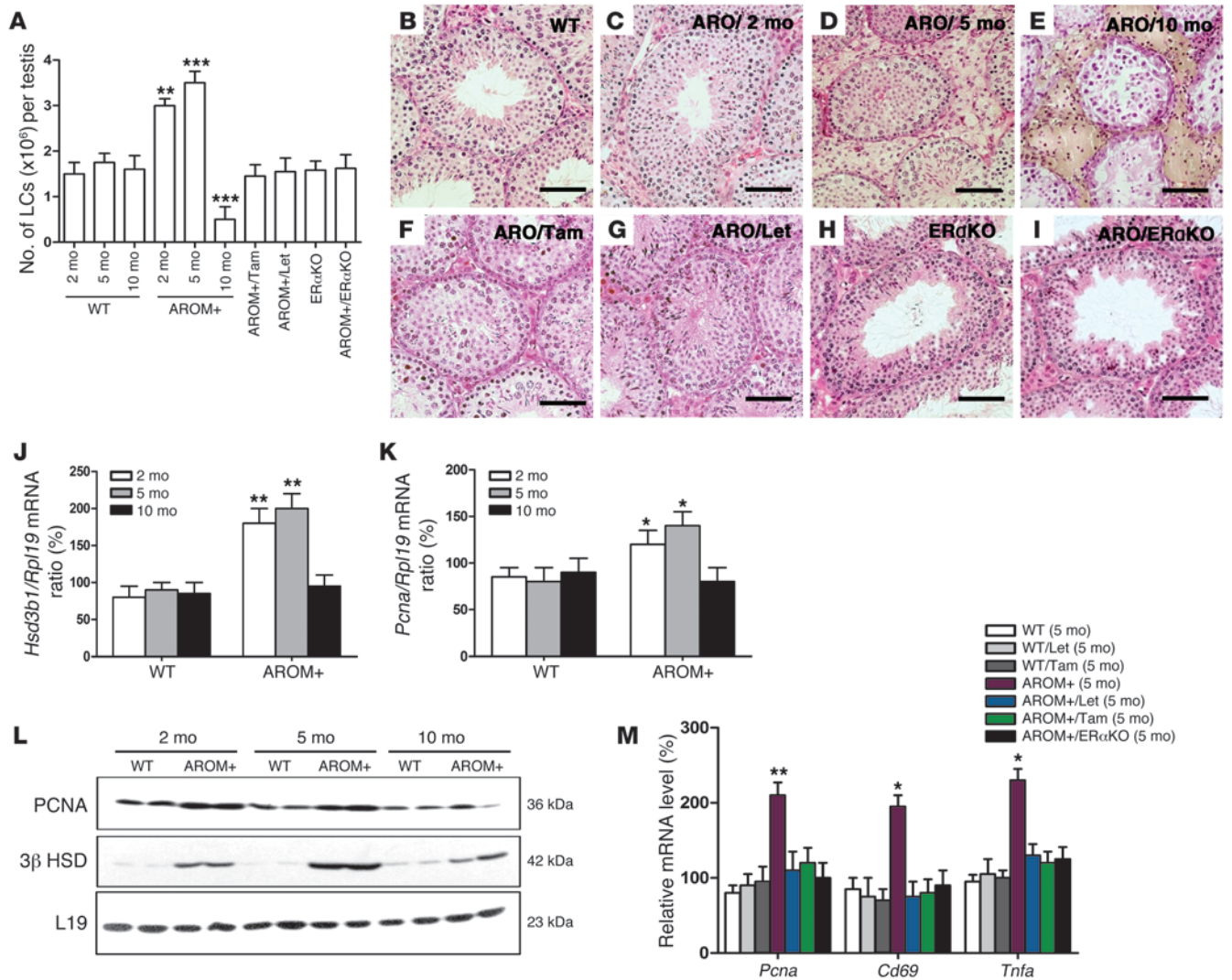
Figure 1
LC hyperplasia and testicular macrophage activation are estrogen/ERα-dependent. (**A**) Total number of LCs per testis in 2-, 5-, and 10-month-old WT and AROM+ males (*n* = 6 per group); AROM+ males treated with letrozole (Let) or tamoxifen (Tam) (*n* = 10 per group); and ERαKO and AROM+/ERαKO males (*n* = 6 per group). (**B–I**) Testicular histopathology. (**B**) WT. (**C**) 2-month-old AROM+. (**D**) 5-month-old AROM+ testis with LC hyperplasia (arrowheads). (**E**) 10-month-old AROM+. Yellowish giant cells (arrow) represent activated testicular macrophages. (**F**) Tamoxifen-treated AROM+. (**G**) Letrozole-treated AROM+. (**H**) ERαKO. (**I**) AROM+/ERαKO. (**J** and **K**) Expression of (**J**) *Hsd3b1* and (**K**) *Pcna* in testes of 2-, 5-, and 10-month-old mice. (**L**) Western blot analysis of PCNA and 3βHSD from testes of 2-, 5- and 10-month-old mice. (**M**) Expression profile of *Pcna*, *Cd69*, and *Tnfa* at testes of 5-month-old WT and AROM+ mice, untreated or treated with letrozole or tamoxifen for 3 months, and 5-month-old AROM+/ERαKO mice. *$P < 0.05$, **$P < 0.01$, ***$P < 0.001$. Scale bars: 50 μm.

Results

LC hyperplasia and testicular macrophage activation are estrogen/ERα dependent. Previously, we reported that the overexpression of *CYP19* in AROM+ mice leads to disrupted spermatogenesis, LC hypertrophy and hyperplasia, and simultaneous activation of testicular macrophages at 4–5 months of age, the result of elevated E2, decreased T, and impaired E2/T ratio (15, 18). Normally, mature LCs do not undergo mitosis beyond 60 days of age in rodents (19). In our AROM+ model, morphometric analysis showed that the number of LCs at 2 and 5 months of age was significantly increased compared with WT mice (*P* < 0.01 and *P* < 0.001, respectively; Figure 1A). Surprisingly, the number of AROM+ LCs

sharply decreased at 10 months compared with 2 and 5 months (*P* < 0.001; Figure 1A). These observations were confirmed by time course histopathology of AROM+ testis at 2, 5, and 10 months. LCs accumulated or hyperproliferated within the interstitium of the AROM+ testis at 2 and 5 months of age (Figure 1, C and D), but were depleted at 10 months of age due to the engulfment of hypertrophic and hyperplastic LCs by activated macrophages (Figure 1E and refs. 15, 18).

To test whether LC hyperplasia in AROM+ testes was directly caused by overexpression of aromatase, and more precisely via the E2/ER-dependent signal pathway, we treated mice either with the aromatase inhibitor letrozole or with the ER antagonist tamoxifen
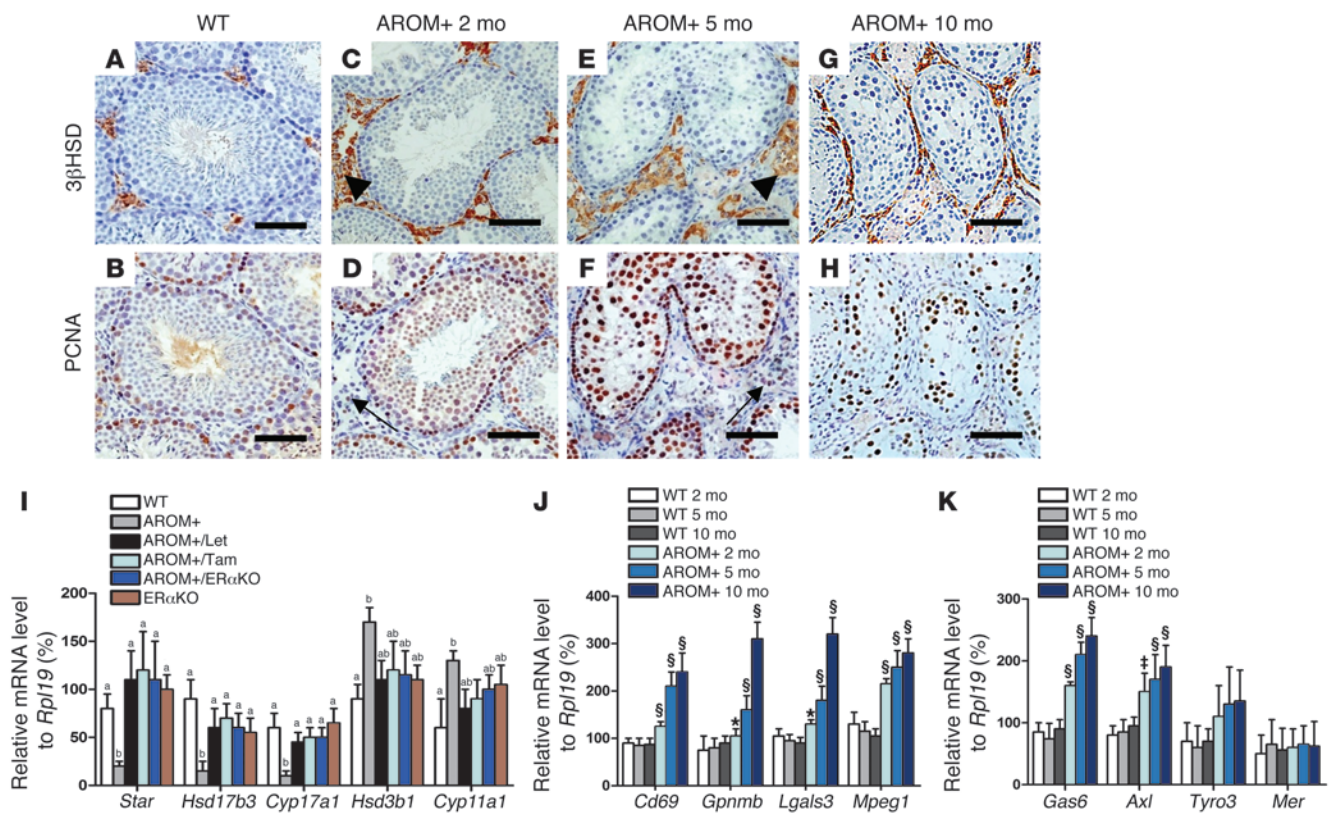
Figure 2
Immunohistochemistry and gene expression profile analysis by qPCR for steroidogenesis and macrophage activation in testes. (**A** and **B**) Immunohistochemical staining for (**A**) 3βHSD and (**B**) PCNA in 2-month-old WT testes. As there were no substantial histological alterations in testis between 2 and 10 months, we used 2-month-old WT testes as controls. (**C**–**H**) 3βHSD (arrowheads) and PCNA (arrows) in LCs in testes of AROM+ mice at 2 (**C** and **D**), 5 (**E** and **F**), and 10 (**G** and **H**) months of age. (**I**) Gene expression of *Star*, *Cyp17a1*, *Hsd17b3*, *Hsd3b1*, and *Cyp11a1* in 5-month-old WT, AROM+ (untreated or treated with tamoxifen or letrozole for 3 months), and AROM+/ERαKO males (*n* = 6 per group). Significant differences between groups (*P* ≤ 0.05) are denoted by different letters above the bars. (**J** and **K**) Age-dependent expression of *Cd69*, *Gpnmb*, *Lgals3*, *Mpeg1*, *Gas6*, *Axl*, *Tyro3*, and *Mer* in WT and AROM+ males at 2, 5, and 10 months of age. *$P < 0.05$, ‡$P < 0.01$, §$P < 0.001$ vs. age-matched WT. Scale bars: 50 μm.

and crossbred the AROM+ mice with ERαKO mice to rescue their testis phenotype as a control (AROM+/ERαKO mice; Figure 1I).

LC numbers were significantly decreased and normalized after 3 months of tamoxifen and letrozole treatment, and testes of 5-month-old AROM+ mice were similar to those of WT and/or AROM+/ERαKO mice (*P* < 0.01; Figure 1, A, B, and F–I), which indicated that chronic exposure to E2 (and an increased E2/T ratio) induced ERα-dependent LC hyperplasia. LC hyperplasia was further confirmed by mRNA expression, Western blot, and IHC assays for hydroxy-Δ-5-steroid dehydrogenase, 3β- and steroid Δ-isomerase 1 (3βHSD; encoded by *Hsd3b1*) and proliferating cell nuclear antigen (PCNA; encoded by *Pcna*) in adjacent slides to visualize colocalization of LCs and PCNA in testis (Figure 1, J–L, and Figure 2, A–H). Furthermore, expression levels of *Pcna* and the macrophage activation markers *Cd69* and *Tnfa* were significantly decreased after 3 months of letrozole or tamoxifen treatment in AROM+ mice, comparable to AROM+/ERαKO and WT controls (Figure 1M). Treatment with letrozole or tamoxifen for 3 months did not have any consequences on testicular histopathology in WT mice (Supplemental Figure 1; supplemental material available online with this article; doi:10.1172/JCI59901DS1).

The expression profile of steroidogenic enzymes, including *Star*, *P450scc*, *Cyp11a1*, *Hsd3b1*, *Cyp17a1*, and *Hsd17b3*, was altered in AROM+ testis cells, but was normalized after letrozole or tamoxifen treatment and in AROM+/ERαKO mice (Figure 2I). Serum E2 levels were significantly elevated in 2- and 5-month-old AROM+ mice, while serum T levels were inversely correlated with E2 levels and were significantly decreased in AROM+ males compared with age-matched male WT controls (Table 1). After 3 months of letrozole or tamoxifen treatment, 5-month-old AROM+ males had significantly elevated serum T and decreased E2 compared with 5-month-old AROM+ or the AROM+ control (oil), but there were no significant changes in drug-treated WT males compared with WT oil control (Table 2).

Novel genes in the E2/ER pathway are involved in testicular macrophage activation and LC hyperplasia in AROM+ males. From cDNA microarray analyses on an Agilent platform, comparing testes of 5-month-old AROM+ with age-matched WT mice, we obtained a list of the 200 most upregulated or downregulated candidate genes on the basis of fold change compared with WT. We used the Ingenuity (IPA) bioinformatics tool to select classified genes with changes greater than 2.0-fold (see Supplemental Table 1 for upregulated and downregu-

Table 1

Serum T and E2 levels in male mice

	2 months		5 months		10 months	
	WT	AROM+	WT	AROM+	WT	AROM+
T (ng/ml)	1.8 ± 0.32	0.29 ± 0.33[A]	6.5 ± 4.71	0.46 ± 0.35[A]	7.87 ± 5.41	0.41 ± 0.45[A]
E2 (pg/ml)	8 ± 1.4	88 ± 32[A]	13 ± 1.9	120 ± 36.2[A]	9.5 ± 1.6	133 ± 32[A]

Values are mean ± SEM (n = 6 per group). [A]P < 0.05 vs. WT.

lated genes). To validate the microarray data, we performed qPCR analysis using testes from 2-, 5-, and 10-month-old AROM+ mice (Figure 2, J and K). The significantly upregulated mRNA of *Gas6*, a chemoattractant that bridges phagocytes to their target cells, in AROM+ versus WT testes was particularly interesting (Supplemental Table 1 and Figure 2K). As indicated by the microarray analysis and validated by qPCR, *Gas6* and several genes involved in macrophage activation, such as *Cd69*, *Gpnmb*, *Lgals3*, *Mpeg1*, and *Axl* (one of the TAM receptors for macrophage), were elevated (Figure 2, J and K). No significant alterations were observed in 2 other TAM receptors, *Tyro3* and *Mer* (Figure 2K). To demonstrate LC- and/or macrophage-specific impairments in testis, we visualized testicular comarkers by immunofluorescence analyses. Double immunostaining of the LC marker 3βHSD and the macrophage marker F4/80 showed that 90% of the interstitial cells were positive for 3βHSD, and less than 10% were positive for F4/80 (Figure 3A). These markers showed the distinct localization of the 2 different testicular cell types in WT and AROM+ mice. Next, we performed double immunofluorescence analysis of 3βHSD and GAS6 in testis. We observed abundant GAS6-immunoreactive staining localized in the plasma membrane and cytoplasm of AROM+ LCs, but we did not find GAS6 in WT testes (Figure 3B). As GAS6 binds to TAM receptors, we examined the protein expression and distribution of TAM receptors in WT and AROM+ testes. To check the colocalization of TAM and macrophages in AROM+ testis, we performed double immunofluorescence analysis of AXL, MER, and TYRO3 versus F4/80 (Figure 3, C–E). Weak AXL staining was observed in WT testicular macrophages, whereas strong AXL signals were present in the plasma membrane and cytoplasm of AROM+ testicular macrophages (Figure 3C). In contrast, weak MER and TYRO3 signals were observed only on the membrane of macrophages in AROM+ testes (Figure 3, D and E). Using a modified isolation and purification protocol for LCs (20), we recovered a population of LCs with 85%–90% purity. Western blot analysis further confirmed our observations and demonstrated that AXL, MER, and TYRO3 were substantially upregulated in AROM+ versus WT macrophages, whereas only trace amounts of TAM receptors, or none at all, were detected in WT and AROM+ LCs (Figure 3F).

E2 upregulates GAS6 expression in LCs and subsequently activates macrophages in vitro through ERα. GAS6 is involved in the recruitment of activated macrophages for phagocytosis (4). As AROM+ testes had highly elevated levels of GAS6, we tested in vitro whether E2/ER was involved in and/or induced by the production of GAS6 in mLTC-1 cells and in LCs isolated from ERαKO testes. Treatment with E2 and the ERα-

selective agonist PPT elevated *Gas6* mRNA levels compared with untreated control in mLTC-1 cells in vitro (Figure 4A). Moreover, addition of the ER antagonist ICI to E2 blocked GAS6 upregulation (P < 0.05, E2 plus ICI vs. E2 or PPT alone; Figure 4A). The ERβ-selective agonist DPN did not cause any changes at the mRNA level (Figure 4A). There were no significant changes in isolated ERαKO LCs (Figure 4A). Moreover, E2 treatment resulted in upregulated *Pcna* expression in mLTC-1 cells, an effect that was blocked by addition of ICI (Figure 4B). E2 treatment did not have any effect on *Pcna* expression in isolated LCs from testes of ERαKO mice (Figure 4B), further confirming the involvement of ERα signaling in this process. GAS6 upregulation was confirmed by immunohistochemistry and immunofluorescence assays in the mLTC-1 cells: upon E2 treatment, 30% of mLTC-1 cells exhibited GAS6 expression in their membranes and cytoplasm (Figure 4, C–F).

The E2- and PPT-induced upregulation of GAS6 observed in LCs (Figure 4, A and C–F) suggested that *Gas6* is a direct target gene of ERα signaling. Therefore, we analyzed transactivation of the *Gas6* promoter by E2. We cotransfected mLTC-1 cells with a construct harboring firefly luciferase under the *Gas6* promoter and a human ERα expression plasmid, according to a previously described method (21), and treated the transfected cells with E2, PPT, or E2 and ICI combined. E2 and PPT treatment increased promoter activity 2-fold compared with controls (Figure 4G). ICI blocked the E2-induced transactivation of the *Gas6* promoter, which suggests that the *Gas6* promoter has a functional estrogen response element. In contrast, DPN treatment did not affect *Gas6* promoter activity, which indicates that *Gas6* promoter transactivation is not mediated by ERβ. As E2 and PPT treatment showed no effects on *Gas6* mRNA levels in ERαKO LCs (Figure 4A), we concluded that the E2-mediated GAS6 upregulation occurred through ERα.

Activation of macrophage cells is mediated through ERα in vitro. To test whether macrophage activation was induced by estrogen/ERα, we treated the RAW246.7 macrophage cell line with E2, PPT, and DPN (Figure 4, H–M). E2 and PPT treatment upregulated expression of *Esr1* and of macrophage activation-associated genes, including *Cd69*, *Tnfa*, *Il6*, *Ccl2*, and *Axl* (Figure 4, H–M). The upregulated expression of these genes was blocked by ICI (P < 0.05, E2 plus ICI vs. E2 or PPT alone; Figure 4, H–M). DPN treatment had no effect on the expression levels of these genes. Moreover, the addition of E2, ICI, and PPT to ERαKO mouse macrophages did not significantly alter *Esr1*, *Cd69*, *Tnfa*, *Il6*, *Ccl2*, or *Axl* (Figure 4, H–M), further demonstrating the role of ERα in macrophage activation.

Table 2

Serum T and E2 levels after letrozole or tamoxifen treatment

	AROM+			WT		
	Vehicle	Letrozole	Tamoxifen	Vehicle	Letrozole	Tamoxifen
T (ng/ml)	0.39 ± 0.42	7.1 ± 4.2[A]	6.4 ± 3.32[A]	7.5 ± 4.3	12.4 ± 3.7	8.1 ± 4.7
E2 (pg/ml)	129 ± 25	8.8 ± 2.0[A]	12 ± 3.4[A]	10.2 ± 2.4	7.7 ± 2.6	8.2 ± 1.8

5-month-old male mice were treated with vehicle, letrozole, or tamoxifen for 3 months. Values are mean ± SEM (n = 6 per group). [A]P < 0.05 vs. WT.
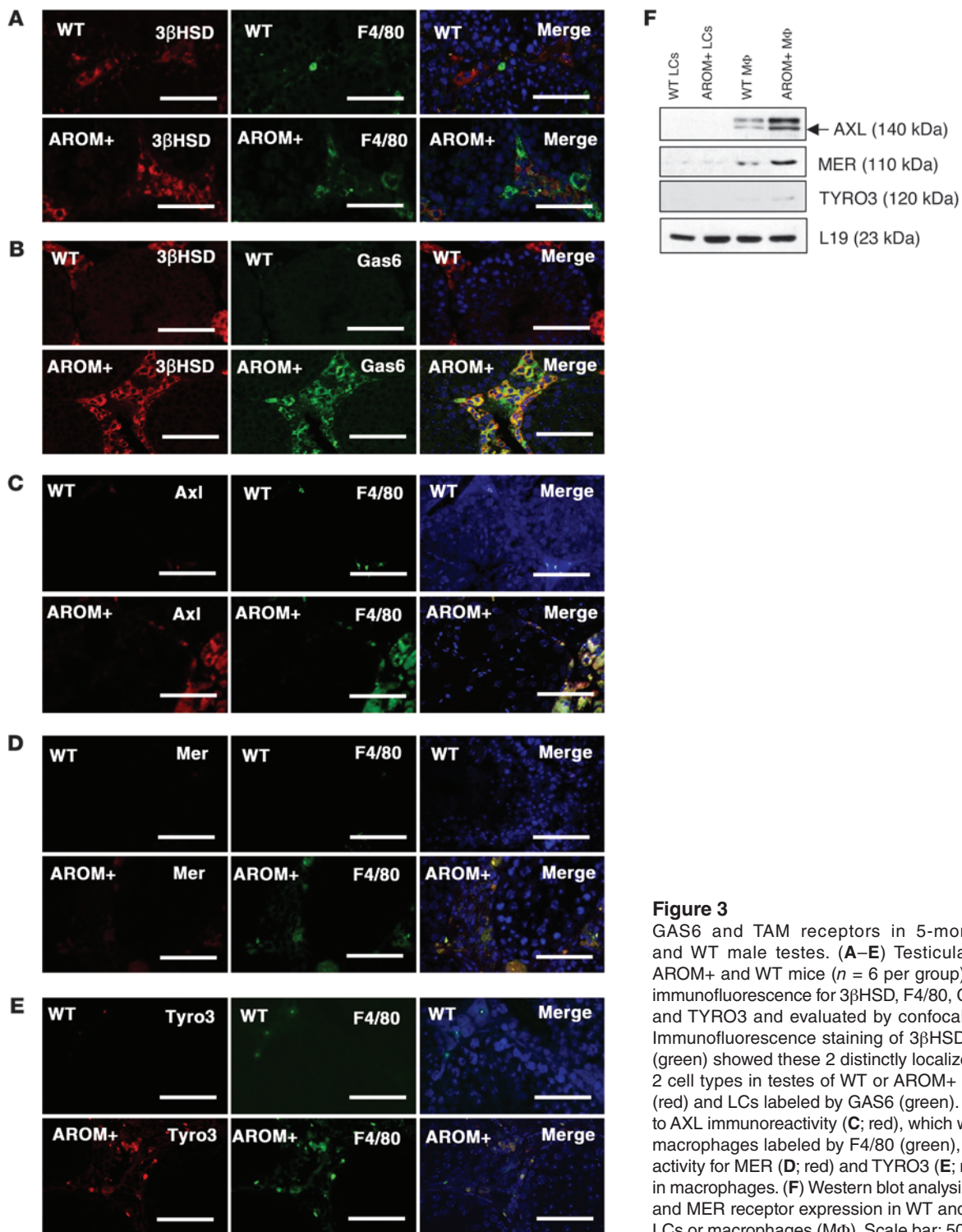
Figure 3
GAS6 and TAM receptors in 5-month-old AROM+ and WT male testes. (**A**–**E**) Testicular sections from AROM+ and WT mice (n = 6 per group) were stained by immunofluorescence for 3βHSD, F4/80, GAS6, AXL, MER, and TYRO3 and evaluated by confocal microscopy. (**A**) Immunofluorescence staining of 3βHSD (red) and F4/80 (green) showed these 2 distinctly localized markers in the 2 cell types in testes of WT or AROM+ mice. (**B**) 3βHSD (red) and LCs labeled by GAS6 (green). (**C**–**E**) In contrast to AXL immunoreactivity (**C**; red), which was colocalized in macrophages labeled by F4/80 (green), weak immunoreactivity for MER (**D**; red) and TYRO3 (**E**; red) was detected in macrophages. (**F**) Western blot analysis of TYRO3, AXL, and MER receptor expression in WT and AROM+ purified LCs or macrophages (MΦ). Scale bar: 50 μm.

E2 induces ERα-dependent, but apoptosis-independent, exposure of PS on the surface of LCs. PS exposure on the cell surface is an important signal for phagocytosis as well as for apoptotic cells (22). PS also acts as a ligand for GAS6 (4). We further tested whether the E2/ERα- and GAS6-dependent AROM+ LC engulfment by macrophages in the AROM+ testis is dependent on PS. First, we tested whether estrogen induced PS exposure on the surface of LCs in vitro by

annexin V staining, because annexin V binds to PS in a quantitative manner (22) and thereby reflects the extent of exposure. E2 treatment induced 20-fold higher PS exposure on the surface of mLTC-1 cells compared with vehicle-treated controls (Figure 5, A and B). The annexin V+ cells were propidium iodide negative (PI−), which suggests that these cells were nonapoptotic. In fact, annexin V+ cells grew as efficiently as the parental annexin V− cells, with a doubling
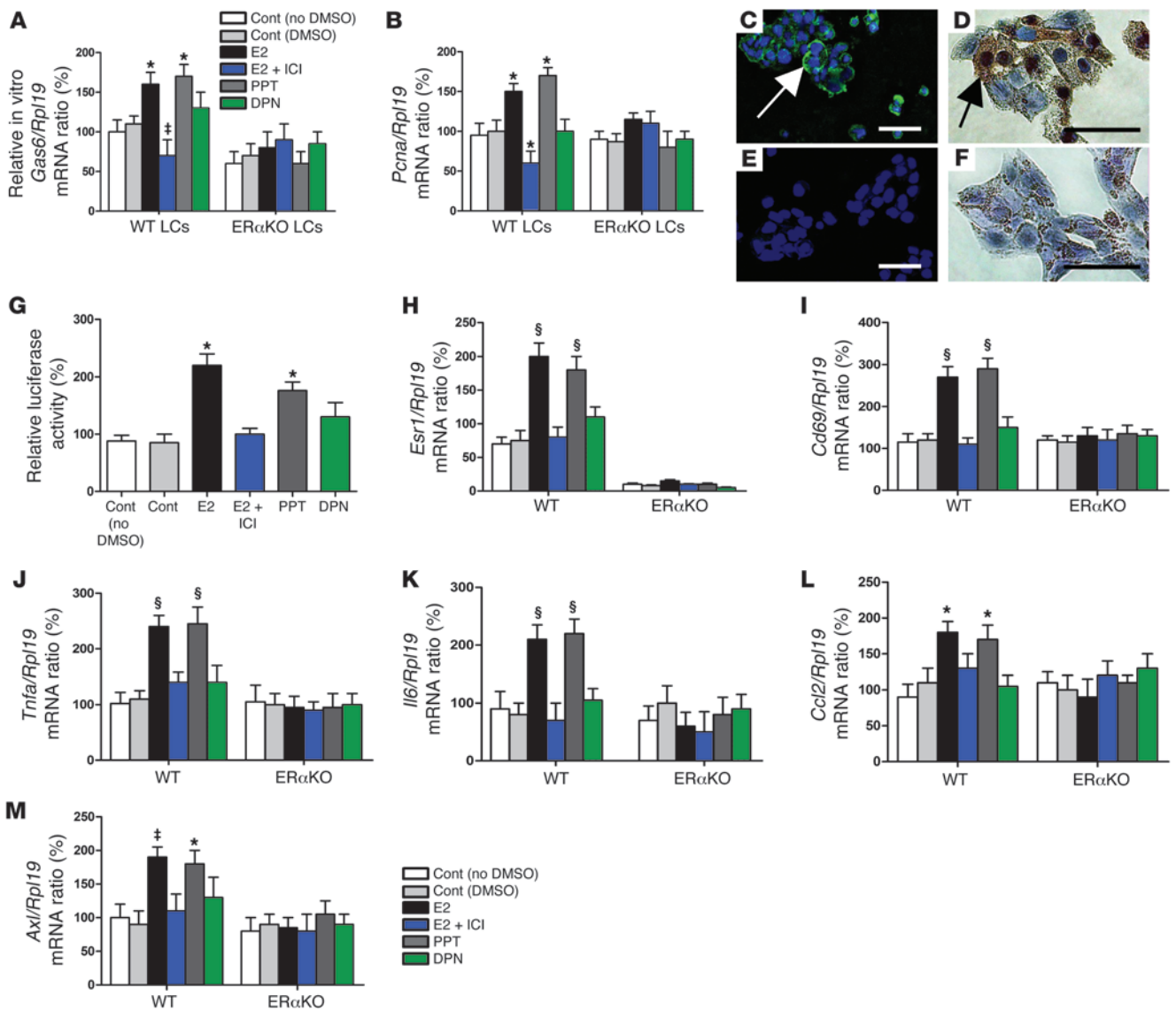
Figure 4

E2/ERα signaling effects on *Gas6* and *Pcna* expression and on macrophage activation markers. (**A** and **B**) mRNA expression of (**A**) *Gas6* and (**B**) *Pcna* in isolated and purified LCs (1.75 × 10⁵ cells/well in 12-well plates) from WT and ERαKO mice, treated or mock-treated with DMSO (controls), 10 nM E2, 10 nM E2 plus 1 μM ICI, 10 nM PPT, or 10 nM DPN for 36 hours. (**C–F**) Immunofluorescent (**C** and **D**) and immunocytochemical (**E** and **F**) analyses for GAS6 staining (arrow) in mLTC-1 cells in vitro. **D** and **F** are mock E2-treated controls. Scale bars: 50 μm. (**G**) mLTC-1 cells were cotransfected with 1.5 μg of a construct containing firefly luciferase under control of the *Gas6* promoter, 20 ng PCMV-ERα, and 0.1 μg PCMV-β, as well as with 10 nM E2, 10 nM E2 plus 1 μM ICI, 10 nM PPT, and 10 nM DPN as indicated. Luciferase activity was normalized to β-galactosidase activity (internal control) to show the transactivation of the *Gas6* promoter by E2. Results represent the average of 3 independent experiments. (**H–M**) mRNA levels of (**H**) *Esr1*, (**I**) *Cd69*, (**J**) *Tnfa*, (**K**) *Il6*, (**L**) *Ccl2*, and (**M**) *Axl* in macrophages from WT and ERαKO mice treated as in **A** and **B**. Results represent the average of 3 independent experiments normalized to *Rpl19*. *$P < 0.05$, ‡$P < 0.01$, §$P < 0.001$ vs. control.

time of 38 ± 1.5 hours, and also went through normal mitosis (Figure 5C). Only a small percentage of the cells were positive for both annexin V and PI, similar to the vehicle-treated control. Moreover, the annexin V⁺PI⁺ cells went through apoptosis, a natural occurrence in vitro. We also found significantly higher *Pcna* expression in E2-treated annexin V⁺ LCs compared with the control, and this increased expression was blocked by addition of ICI (Figure 5D).

Mitochondrial membrane potential (MMP) is an important parameter of mitochondrial function, membrane integrity, and

energy coupling and is also an early marker for apoptosis (23). To determine whether the estrogen-induced PS exposure on the surface of LCs was a downstream effect of the cells undergoing apoptosis, we measured the relative MMP of these cells upon E2 treatment. We did not observe any significant MMP changes in E2-treated annexin V⁺PI⁻ mLTC-1 cells (Figure 5E), which may indicate that the cells were nonapoptotic and that PS exposure was independent of programmed cell death. E2 treatment did not have any effect on PS exposure on the cell surface compared with vehicle treatment in
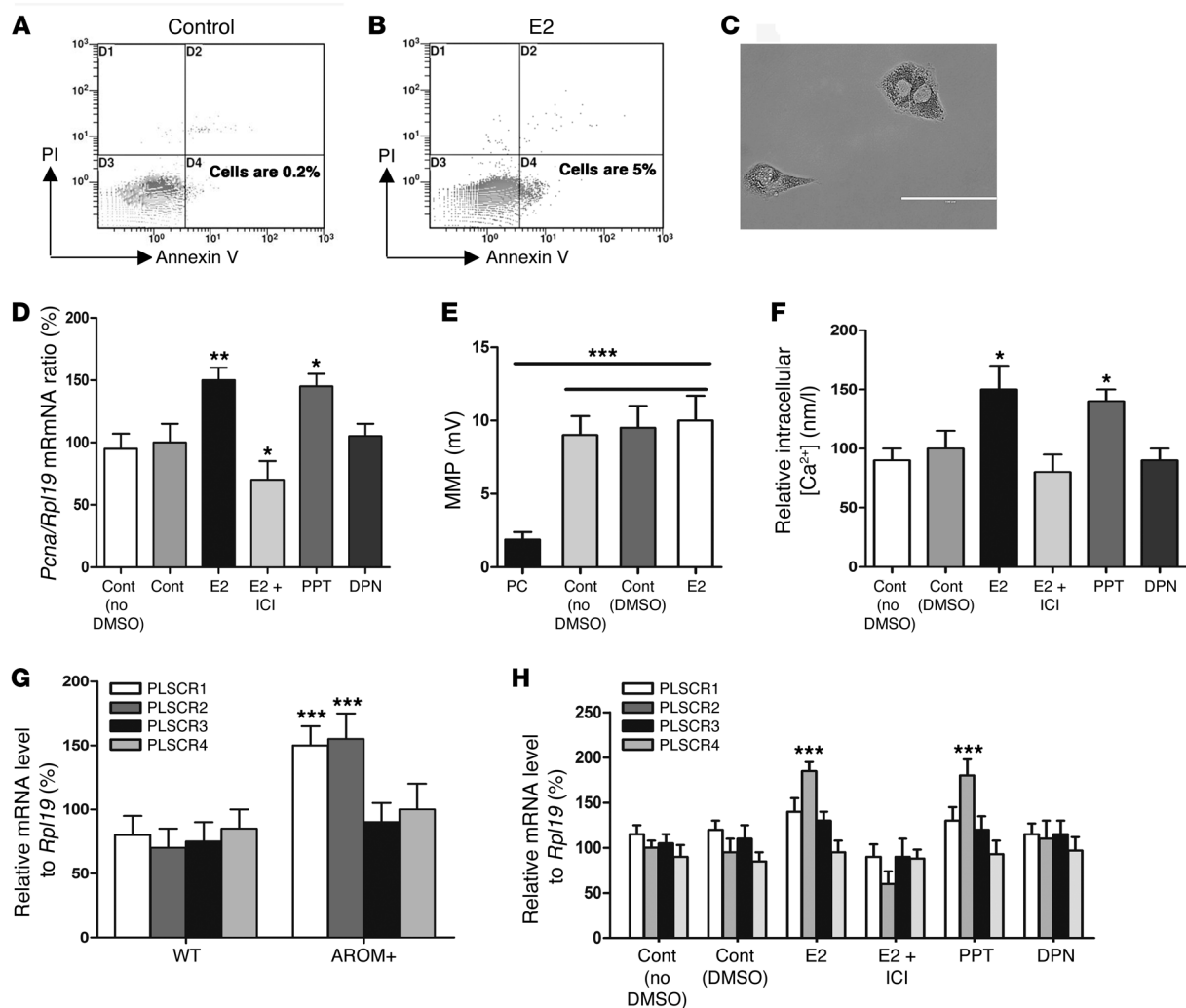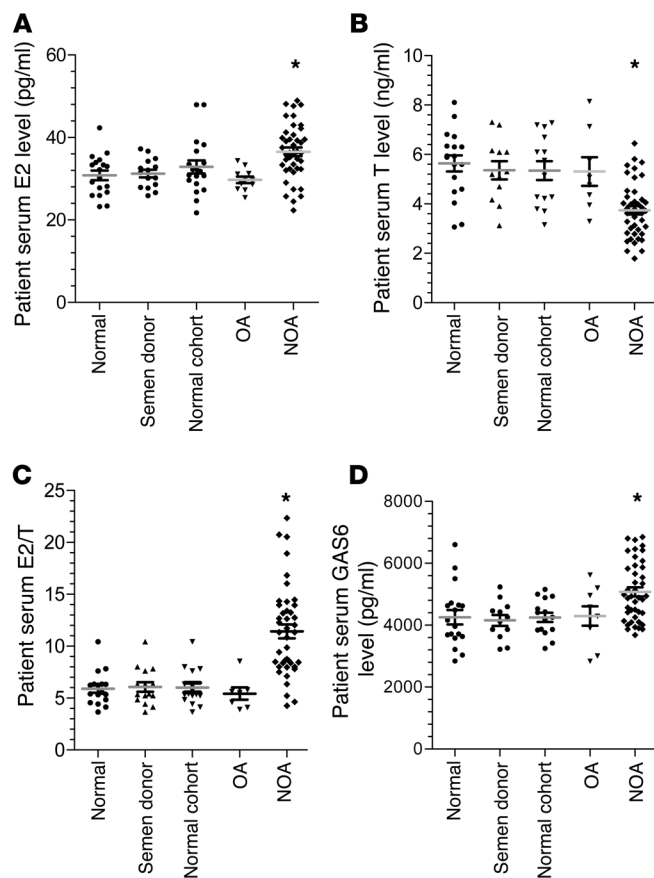
Figure 5
Estrogen effects on PS asymmetry, apoptosis, MMP, cell proliferation, and scramblase expression in AROM+ LCs and in mLTC-1 cells. (**A** and **B**) PS exposure on the surface of mLTC-1 LCs (passage 16) was measured by annexin V–FITC staining (x axis) without (**A**) or with (**B**) 10 nM E2 treatment, and apoptosis was measured by PI staining (y axis). (**C**) Dividing annexin V+ mLTC-1 LCs after E2 treatment were observed by phase-contrast microscopy after 36 hours of incubation at 37°C. Scale bar: 100 μm. (**D**) *Pcna* mRNA levels, normalized to *Rpl19*, in annexin V+ mLTC-1 LCs without (Cont) or with 10 nM E2, 10 nM E2 plus 1 μM ICI, 10 nM PPT, or 10 nM DPN treatment. (**E**) MMP of control (with or without DMSO) or E2-treated mLTC-1 LCs was measured using the JC-1 dye. Phosphatidylcholine-treated cells (PC) were used as positive controls for mitochondrial dissipation. (**F**) Intracellular [Ca^{2+}] in mLTC-1 cells, treated as in **D**, was measured using the Ca^{2+} indicator Fura2/AM. (**G**) *Plscr1–Plscr4* mRNA levels of 5-month-old WT and AROM+ mouse testes, normalized to *Rpl19*. (**H**) *Plscr1–Plscr4* mRNA levels, normalized to *Rpl19*, in mLTC-1 cells treated as in **D**. Each sample was assessed in triplicate, and each experiment was repeated 3 individual times. *$P < 0.05$, **$P < 0.01$, ***$P < 0.001$ vs. respective control (no DMSO), or as indicated by brackets.

ERαKO LCs (Supplemental Figure 2), thereby suggesting that the induced PS exposure was a direct effect of E2/ERα signaling.

Estrogen alters phospholipid asymmetry by increased intracellular Ca^{2+} levels and scramblase expression, leading to PS exposure on the surface of AROM+ LCs and mLTC-1 cells. To maintain the natural lipid asymmetry of a normal cell, a group of P-type ATPases (mainly ATP8B3, a flippase that specifically transports PS and phosphatidylethanolamine [PE] inward, and ABCA1, a floppase that pumps phospholipids in an outward direction) actively transports PS and PE from the external leaflet to the internal leaflet of the plasma membrane (24). ATP8B3 and ABCA1 are expressed in the testis (25) and liver (26). We tested whether estrogen exposure affected the expression

of these 2 enzymes in the testes of 2-, 5-, and 10-month-old WT and AROM+ mice as well as in mLTC-1 cells treated with E2, E2 and ICI combined, PPT, and DPN. No significant differences in *Atp8b3* and *Abca1* mRNA levels were found between AROM+ and WT mice or among different treatments in mLTC-1 cells (Supplemental Figure 3, A and B). An increase in intracellular [Ca^{2+}], either due to transcriptional activation or the exposure of cells to environmental stress, activates phospholipid scramblases (PLSCRs), leading to the loss of membrane asymmetry (27–29). Therefore, we tested whether intracellular [Ca^{2+}] levels mediate this upregulation process. E2 and PPT treatment significantly upregulated intracellular [Ca^{2+}] levels compared with control treatment in mLTC-1 cells (Figure 5F). This

A

B

C

D

Figure 6
Serum steroid hormone and GAS6 levels from infertile men and normal control male patients. (**A**–**D**) Serum levels of (**A**) E2, (**B**) T, and (**D**) GAS6 and (**C**) the E2/T ratio from NOA infertile men ($n = 42$), OA infertile men ($n = 11$), and 3 control groups: normal healthy men with children ($n = 18$), healthy semen donors ($n = 12$), and a normal cohort of healthy volunteers ($n = 15$). *$P \leq 0.05$ vs. all other groups.

giant cell is the macrophage, and the viable LCs are labeled in green and additionally identifiable by the rapid movement of their filopodial protrusions. WT LCs were not engulfed by phagocytes, and rapid engulfment occurred only in AROM+ LCs at 10 hours (Supplemental Videos 1 and 2 and Supplemental Figure 5). When we cocultured viable LCs and macrophages from WT testes in vitro and treated them with or without E2, E2 and ICI combined, PPT, or DPN, the phagocytosis of living LCs by macrophages was induced by E2/ERα (Supplemental Figure 5). Phagocytosis was dependent on E2 and ERα action when the WT macrophages and LCs were preincubated with E2 for 4 hours prior to the engulfment assay (Supplemental Video 3 and Supplemental Figure 5). Moreover, preincubation of cells with anti-GAS6, anti–annexin V, or soluble anti-AXL antibodies completely abrogated phagocytosis (Supplemental Videos 4–6), which further confirmed that an AXL-GAS6-PS complex mediates the bridging of LCs to phagocytes.
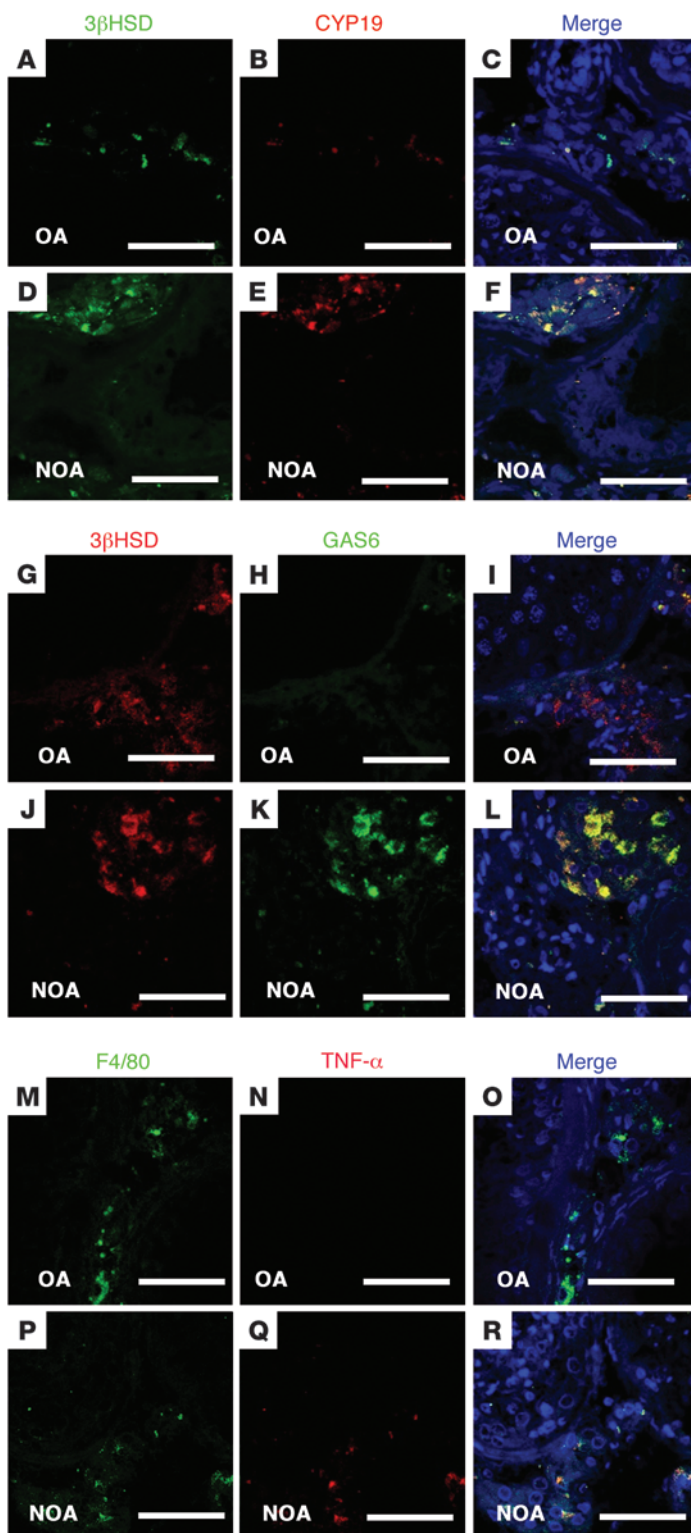
Molecular changes in the testes of a subset of infertile men are similar to the AROM+ mice phenotype. To test whether this AROM+ mouse model reflects human male infertility, we measured steroid hormones and GAS6 expression in patient serum and testes, respectively. Significantly elevated serum E2 and GAS6 levels, decreased T levels, and an increased E2/T ratio were found in NOA infertile subjects ($n = 42$) compared with obstructive azoospermia (OA) infertile subjects ($n = 11$) and normal healthy Chinese men with children ($n = 18$) (Figure 6, A–D). Serum E2, T, GAS6, and E2/T ratio values from normal healthy Chinese men with children did not differ significantly from those of 2 additional control groups: healthy men who were semen donors ($n = 12$), and a normal cohort of healthy male volunteers ($n = 15$) (Figure 6, A–D). We observed abundant and stronger expression of CYP19, GAS6, and TNF-α proteins in needle biopsy testicular samples from Chinese men with NOA ($n = 20$) compared with OA controls ($n = 10$) by immunofluorescence analysis (Figure 7, A–R). Next, we validated the selected important genes found in AROM+ mice by cDNA microarray and qPCR on testicular biopsies of OA ($n = 47$) and NOA ($n = 11$) infertile Japanese patients. We found significantly elevated *CD69*, *TNFA*, *CYP19*, *GAS6*, *TYRO3*, and *AXL*, but downregulated *HSD17B3* and *MER*, in NOA versus OA testes ($P < 0.01$; Figure 8, A–H). *PLSCR1*, *PLSCR3*, and *PLSCR4* were significantly upregulated, but *PLSCR2* was downregulated, in NOA versus OA testes ($P < 0.001$; Figure 8, I–L). Overall, these results suggested that NOA patients have a pattern of molecular markers rather similar to that of AROM+ mice.

Discussion
We have previously shown that LC hyperplasia appears in AROM+ testes by 4–5 months of age and that LC adenoma appears by 6–8 months (15, 18). No signs of malignancy are observed in testes from aged AROM+ mice (15, 18). Marked activation of testicular macrophages beginning at 4 months, along with subsequent LC depletion, is evident in AROM+ mice (15, 18). In the present

effect was blocked by ICI treatment ($P < 0.05$; E2 plus ICI vs. E2 or PPT alone); however, DPN had no effect (Figure 5F). Next, we measured the levels of *Plscr1*–*Plscr4*, which belong to another class of ATPases involved in the transbilayer movement of plasma membrane phospholipids (30). Significantly elevated levels of *Plscr1* and *Plscr2* were observed in AROM+ versus WT testes (Figure 5G). E2 and PPT treatment of mLTC-1 cells upregulated expression of *Plscr2* (Figure 5H). Although *Plscr1*, *Plscr3*, or *Plscr4* expression was not significantly changed in mLTC-1 cells compared with control, expression of *Plscr1* (E2, $P = 0.016$; PPT, $P = 0.047$) and *Plscr3* (E2, $P = 0.008$; PPT, $P = 0.034$) was significantly elevated compared with combined E2 and ICI treatment (Figure 5H), implicating the activation of *Plscr1* and *Plscr3* upon E2/ERα action. The increase in *Plscr1*, *Plscr2*, and *Plscr3* was blocked by ICI ($P < 0.05$; E2 plus ICI vs. E2 or PPT alone), and DPN treatment did not induce any changes (Figure 5H). Treatment of isolated ERαKO LCs with E2, E2 and ICI combined, and PPT did not have any significant effects on the mRNA levels of *Plscr1*–*Plscr4* (Supplemental Figure 4). Upon E2/ERα induction, Ca^{2+}-mediated upregulation of *Plscr2*, and to some degree *Plscr1* and *Plscr3*, resulted in loss of membrane asymmetry and increased PS exposure on the surface of LCs.

E2-induced GAS6 serves as an engulfment signal on living AROM+ LCs. GAS6 bridges apoptotic cells and macrophages by binding to exposed PS on the apoptotic cell surface and to TAM receptors, such as AXL, on the macrophage plasma membrane (2). We performed 3D live cell imaging of phagocytes that were incubated with living LCs isolated from WT or AROM+ testes (Supplemental Videos 1–3). In the videos, the floating, unlabeled, irregular-shaped

Figure 7
Immunofluorescence analysis of CYP19, GAS6, and TNF-α in testicular biopsies of NOA (n = 20) and OA (n = 10) infertile patients. Shown are OA (**A–C**, **G–I**, and **M–O**) and NOA (**D–F**, **J–L**, and **P–R**) testicular biopsy sample sections stained with anti-3βHSD (**A** and **D**; green) and anti-CYP19 (**B** and **E**; red); with anti-3βHSD (**G** and **J**; red) and anti-GAS6 (**H** and **K**; green); and with anti-F4/80 (**M** and **P**; green) and anti–TNF-α (**N** and **Q**; red). (**C**, **F**, **I**, **L**, **O**, and **R**) Merged images show colocaliztion (yellow); nuclear counterstaining with DAPI (blue). Scale bars: 50 μm.

vented the development of malignancy. By real-time 3D imaging, we monitored E2-induced PS exposure facilitating GAS6 anchoring to the surface of living LCs, which in turn served as an engulfment (i.e., "find-me") signal for E2-activated macrophages, leading to viable LC engulfment.

The membrane lipid asymmetry of mammalian cells is maintained by P-type ATPases of the following 3 types: flippase, floppase, and Ca^{2+}-dependent scramblase (24). Scramblases are of particular interest, as cytoplasmic $[Ca^{2+}]$ increases can activate these enzymes and cause phospholipid asymmetry (31). Increased $[Ca^{2+}]$ levels and the appearance of PS at the cell surface occur in a variety of diseases (7). The present study demonstrated that E2/ERα signaling may result in elevated intracellular $[Ca^{2+}]$ in LCs, which may lead to abnormal Ca^{2+}-dependent scramblase-mediated PS exposure. Although expression of expression of *PLSCR2* has been suggested to be restricted to the testis, *PLSCR1*, *PLSCR3*, and *PLSCR4* are ubiquitously expressed in all tissues, including testis (30). Here, we observed elevated levels of *Plscr1* and *Plscr2* in AROM+ mice and elevated *Plscr2* in mLTC-1 cells. In the testes of NOA infertile men, *PLSCR1*, *PLSCR3*, and *PLSCR4* were elevated, but surprisingly, *PLSCR2* was decreased. For now, we are not able to explain this differential expression pattern of *PLSCR1–PLSCR4* (especially *PLSCR2*) among AROM+ mice, mLTC-1 cells, and NOA men, which needs to be further explored. A plausible explanation for this differential expression could be that some cell- or strain/species-specific *PLSCR1–PLSCR4* expression differences exist between murine and human testis. Transcriptome analysis for *PLSCR2* expression in GEO profiles showed similar *PLSCR2* expression in multiple human tissues (e.g., testis, brain, muscle, and skin); moreover, the expression patterns of *PLSCR2* in normal tissues were different for human and mouse (accession nos. GDS596 and GDS182). This combination effect of elevated *PLSCR* expression would imply that PS exposure is increased on the outer leaflet of LCs. Although PS exposure is an engulfment signal for apoptotic cells (1, 2), we observed that E2-induced PS exposure in LCs was apoptosis independent. Earlier findings of Fricker et al. and Segawa et al., who reported constitutive PS exposure on other viable cells, also support the present results (32, 33). Nevertheless, exposed PS could served as a beacon for specific molecules, such as GAS6 or MFG-E8 (32), leading to the downstream effects. In contrast to the present results, a former study has demonstrated that acute estrogen exposure leads to the ERα-dependent blunting of agonist-induced $[Ca^{2+}]$ responses (34). This discrepancy may be due to the fact that E2/ERα signaling is largely dependent on the recruitment of coactivators or corepressors in different cellular and tissue contexts (35).

study, we demonstrated that E2 or an increased E2/T ratio not only promoted macrophage activation, but also regulated GAS6 production and induced PS exposure on the surface of LCs, in an ERα-dependent manner. This ERα-dependent macrophage activation was independent of apoptosis and led to E2/ERα-mediated phagocytosis. As a consequence, phagocytosis most likely pre-
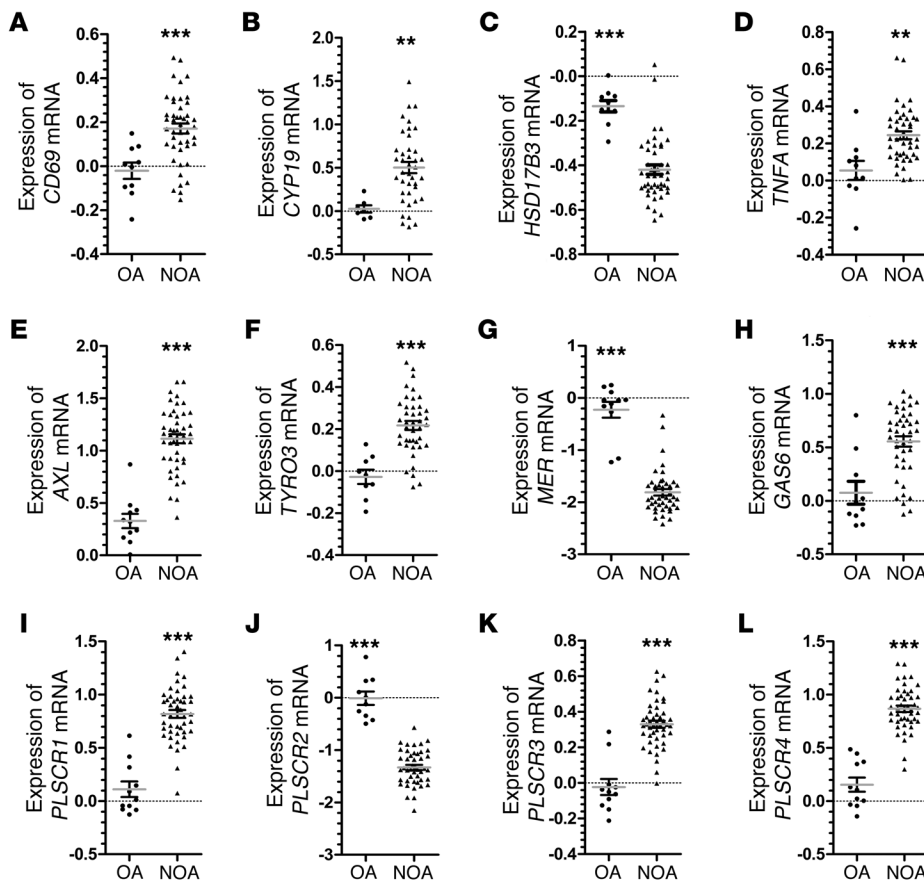
Figure 8
Validation of selected genes identified by AROM+ microarray. qPCR was used to validate (**A**) *CD69*, (**B**) *CYP19*, (**C**) *HSD17B3*, and (**D**) *TNFA*; TAM receptors (**E**) *AXL*, (**F**) *TYRO3*, (**G**) *MER*, and (**H**) *GAS6*; and (**I**–**L**) *PLSCR1–PLSCR4* in testicular needle biopsy samples from OA ($n = 11$) and NOA ($n = 47$) infertile patients. **$P < 0.01$, ***$P < 0.001$ vs. OA.
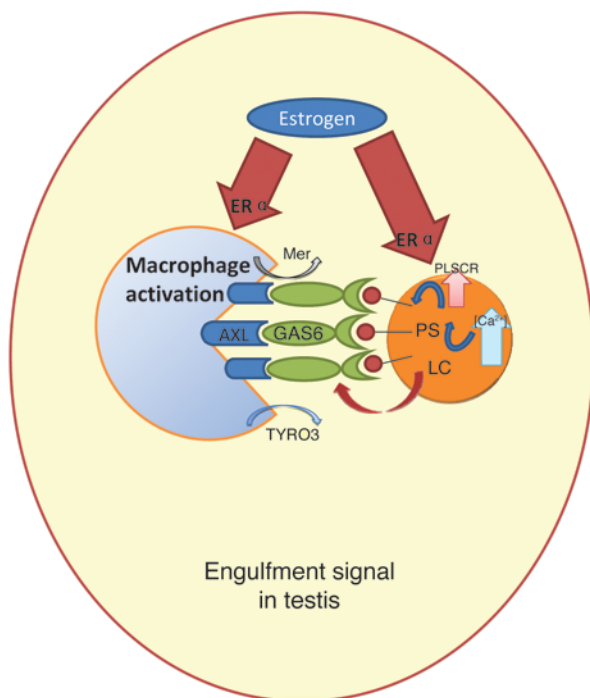
We also observed E2-induced expression of GAS6 and PCNA in AROM+ LCs and mLTC-1 cells, but not in AROM+/ERαKO and ERαKO LCs. We showed that GAS6 upregulation was transcriptionally regulated by E2/ERα signaling. Mo et al. reported that GAS6 expression is ERα dependent (21). Given the role of GAS6 in stimulating the proliferation of several cells (21, 36, 37) and its induction by estrogen, GAS6 has been proposed to be one of the factors involved in estrogen-stimulated autoimmune disorders (36).

Even though testicular tumors are the leading form of cancer in men 20–39 years of age, LC neoplasms account for merely 2%–3% of testicular tumors (38). Previously, our group and another group have shown that chronic estrogen stimulation induces LC hyperplasia and multinucleated giant cells in the testicular interstitium in AROM+ and estrogen sulfotransferase knockout mice (15, 39), but that these cells never develop into LC tumors (15, 39). Our present data provide insight into the molecular mechanisms behind this protection against tumorigenic transformation. A report showing the inactivation of monocytes, macrophages, and neutrophils in a murine ERα conditional knockout model also supports this notion (40). Genes related to macrophage activation, such as *Gpnmb*, *Cd68*, and *Tnfa*, were significantly increased in AROM+ testis and significantly downregulated upon letrozole and tamoxifen treatment and in AROM+/ERαKO mice. These markers of macrophage activation were also significantly increased by E2 and PPT treatment in mLTC-1 cells and blocked by ICI. These findings suggested that the E2-mediated activation of macrophages may be the driving force in preventing testicular tumor formation in AROM+ mice. Therefore, higher estrogen levels may also

be protective against testicular LC tumor formation in humans, albeit at the cost of male fertility.

We previously reported that intratesticular T concentration significantly decreased, and intratesticular E2 concentration significantly increased, in AROM+ males compared with age-matched WT males (41). The low level of intratesticular T was thought to reflect a markedly declined circulating T concentration in AROM+ mice (41, 42), as similar results were also reported previously in men (43). No significant difference was found in serum luteinizing hormone (LH) concentrations between AROM+ and WT males (41, 42). However, there were less individual variations in LH concentration in AROM+ versus WT mice, suggesting the possibility of reduced LH amplitude in AROM+ males (42). Similar effects on LH amplitude have been also reported in men after exogenous estrogen administration (44). We also reported significantly decreased serum follicle-stimulating hormone (FSH) levels in AROM+ males (42), which exert E2 feedback effects on serum FSH, supporting the hypothesis that estrogens suppress FSH secretion in males (45, 46). It seems that, despite normal serum LH concentrations, androgen levels were reduced significantly in AROM+ mice, which supports the idea of testicular failure in AROM+ mice.

TYRO3, MER, and AXL are differentially expressed in LCs, Sertoli cells, and testicular macrophages, respectively (47). GAS6 binds to these TAM receptors with markedly different affinities (AXL≥TYRO3>>MER) (2), and GAS6 binds to AXL-Fc, TYRO3-Fc, and MER-Fc at 0.4, 2.7, and 29.0 nM, respectively (48). It is highly likely that AXL may be the favored receptor of GAS6 in vivo. The present data from AROM+ mice and NOA infertile men

Figure 9
Possible mechanism of estrogen/ERα-mediated engulfment of LCs by testicular macrophages. Binding of estrogen to its receptor, ERα, in testicular macrophages induces their activation, resulting in CD69 and TNF-α production and TAM receptor expression on the macrophage cell surface. Simultaneously, in LCs, E2/ERα signaling increases soluble GAS6 production and intracellular [Ca^{2+}], which in turn induces PS exposure independent of apoptosis. Next, GAS6 is anchored on the surface of LCs by binding to the exposed PS and serves as an engulfment signal mainly for AXL on E2-activated macrophages. Finally, the formation of an AXL-GAS6-PS complex leads to the phagocytosis of LCs by testicular macrophages.

demonstrated that AXL was preferentially upregulated in testes. Furthermore, we showed via real-time 3D imaging assay that pre-incubation of LCs and macrophages with anti-AXL, soluble GAS6, and anti-GAS6 antibodies fully blocked phagocytosis, even upon E2 treatment. Therefore, we concluded that increased E2 and/or an increased E2/T ratio induced testicular macrophages to engulf viable LCs, predominantly via an AXL-GAS6 interaction. Accordingly, we detected increased levels of *CYP19*, *GAS6*, *PLSCRs*, and *CD69* in NOA patients compared with OA controls. An important caveat to consider when using OA infertile men as a control is the potential underestimation of the alterations in gene expression. We demonstrated the significantly increased levels of *CYP19*, *GAS6*, and *CD69* in the testicular biopsies of NOA infertile men, in concert with the increased serum E2/T ratio in infertile men with elevated serum levels of GAS6. Collectively, these results suggest that GAS6 is a strong potential clinical biomarker for male infertility detection. These preliminary findings highlight the need for a large-scale clinical investigation of GAS6 in infertile men.

Taken together, our present findings are indicative of possible molecular mechanisms underlying estrogen-mediated LC hyperplasia and the subsequent macrophage engulfment process (Figure 9). In addition to their crucial role in reproduction, E2 and ERα influence numerous inflammatory responses (49, 50). Moreover, macrophages play a pivotal role in the modulation of immune responses by E2 (40, 51, 52). LCs express abundant ERα and GAS6 (21, 53). In the present study, we demonstrated that E2/ERα promoted LC hyperplasia and GAS6 production, transactivation of the *Gas6* promoter by E2 through ERα and Ca^{2+}-dependent PS exposure on the surface of LCs. Simultaneously, we showed that E2/ERα activated macrophages. The subsequent interaction among GAS6, LCs, and testicular macrophages resulted in the formation of an AXL-GAS6-PS complex that led to LC engulfment. Moreover, by 3D real-time imaging, we confirmed that E2 pro-

motes macrophage activation via ERα signaling, and the E2/ERα-activated macrophages engulf the living LCs via the AXL-GAS6-PS interaction. This mechanistic series of events maintains a finely tuned balance between testicular macrophages and LCs. Consequently, the depletion of testosterone-producing LCs resulted in disrupted spermatogenesis, thereby leading to male infertility. Our findings suggest a novel potential application of GAS6 as a clinical biomarker for male infertility and as a possible therapeutic for a subset of infertile men with an impaired E2/T ratio.

Methods

Further information can be found in Supplemental Methods.

Mouse studies. AROM+ and ERαKO mice (both C57BL/6 genetic background) have been described previously (18, 54). Mice had free access to soy-free chow (SDS RM-3; Whitham) and tap water ad libitum and were handled in accordance with the animal care policies of Chinese Agricultural University. WT and AROM+ mice were sacrificed at similar ages (2, 5, and 10 months; *n* = 6 per group), anesthetized by i.p. injection of 200 μl of 1% Avertin. Blood was collected by cardiac puncture, and tissues were dissected for macroscopic analyses. For the drug treatment studies, 2-month-old male AROM+ and age-matched WT mice (*n* = 10 per group) were randomly assigned into groups, fed soy-free chow, and s.c. injected once daily with vehicle (corn oil), 2.0 mg/kg/d letrozole, or 0.4 mg/kg/d tamoxifen for 90 days. ERαKO and AROM+/ERαKO mice (*n* = 6 per group) were used for isolation of testicular LCs and macrophages. We used cDNA microarray analyses on an Agilent platform to determine transcriptional changes in the testes of 5-month-old AROM+ mice compared with age-matched WT mice. Microarray data for mouse studies were deposited in GEO (accession no. GSE55254).

Human testicular and serum studies. Microarray analysis was performed on testicular biopsy specimens from Japanese patients with NOA (*n* = 47; aged 24–52 years) and OA (*n* = 11; aged 22–57 years). Microarray data for human studies were deposited in GEO (accession no. GSE9210). Immunohistochemical analysis was performed on testicular biopsy specimens obtained from Chinese patients with NOA (*n* = 20; aged 28–45 years) and OA (*n* = 10; aged 24–40 years). Additionally, serum samples were obtained from normal healthy Chinese men with children (*n* = 18), healthy men who were semen donors (*n* = 12), a normal cohort of healthy volunteers (*n* = 15; aged 20–45 years), Chinese patients with NOA (*n* = 42; aged 22–45 years), and Chinese patients with OA (*n* = 11; aged 24–40 years). The definition of OA and NOA and the biopsy analysis were as previously described (55). Due to the difficulties in obtaining normal human testicular samples, biopsies from the OA infertile men served as controls for the NOA cases. Briefly, the testicular biopsies for microarray analysis and immunohistochemical examination included a minimum of 3 biopsies per individual, and multiple unilateral testicular sites were sampled from each individual. Furthermore, each patient went through testicular sperm extraction for assisted reproduction and/or diagnostic biopsy for histological evaluation. The histology of OA

patients revealed the presence of germ cells at all stages of spermatogenesis. In contrast, NOA patients had defects in spermatogenesis, and the degree of spermatogenic defects in NOA patients was histologically evaluated according to Johnsen's scoring (56). The average Johnsen's scores in the NOA and OA groups ranged 1–6.5 and 5.1–9, respectively.

Statistics. Data were analyzed for statistical significance with SPSS 12.0.1. Data for all groups were first tested for normality with the Shapiro-Wilk test. If the group data were normally distributed, they were compared using 1-way ANOVA. CI for means was 95%. Logarithmic transformations were carried out for analysis of groups with non-Gaussian distributions. All numerical data are presented as mean ± SEM. A *P* value less than 0.05 was considered significant. All graphs were generated with GraphPad Prism 5.0 (GraphPad Software Inc.).

Study approval. The Ethics Committee for Animal Experimentation of China Agricultural University (Beijing, China) approved all animal experiments (approval no. SKLAB2010-01-03). All studies involving human subjects were performed with approval from the Ethics Committees of Niigata University (Niigata, Japan), Tachikawa Hospital (Tachikawa, Japan), St. Mother Hospital (Fukuoka, Japan), Tokai University (Tokyo, Japan), and 306th Hospital of PLA (Beijing, China), and study participants provided written informed consent.

Address correspondence to: Xiangdong Li, State Key Laboratory of Agrobiotechnology, College of Biological Sciences, China Agricultural University, Beijing 100193, People's Republic of China. Phone: 86.10.62734389; Fax: 86.10.62734389; E-mail: xiangdongli@cau.edu.cn. Or to: George F. Gao, CAS Key Laboratory of Pathogenic Microbiology and Immunology (CASPMI), Institute of Microbiology, Chinese Academy of Sciences, Beijing 100101, People's Republic of China. Phone: 86.10.64807688; Fax: 86.10.64807882; E-mail: gaof@im.ac.cn.

1. Ravichandran KS. Find-me and eat-me signals in apoptotic cell clearance: progress and conundrums. *J Exp Med*. 2010;207(9):1807–1817.
2. Lemke G, Rothlin CV. Immunobiology of the TAM receptors. *Nat Rev Immunol*. 2008;8(5):327–336.
3. Hanayama R, et al. Autoimmune disease and impaired uptake of apoptotic cells in MFG-E8-deficient mice. *Science*. 2004;304(5674):1147–1150.
4. Scott RS, et al. Phagocytosis and clearance of apoptotic cells is mediated by MER. *Nature*. 2001; 411(6834):207–211.
5. Hanayama R, Tanaka M, Miwa K, Shinohara A, Iwamatsu A, Nagata S. Identification of a factor that links apoptotic cells to phagocytes. *Nature*. 2002; 417(6885):182–187.
6. Elliott MR, Ravichandran KS. Clearance of apoptotic cells: implications in health and disease. *J Cell Biol*. 2010;189(7):1059–1070.
7. Zwaal RF, Comfurius P, Bevers EM. Surface exposure of phosphatidylserine in pathological cells. *Cell Mol Life Sci*. 2005;62(9):971–988.
8. Jacobo P, Guazzone VA, Theas MS, Lustig L. Testicular autoimmunity. *Autoimmun Rev*. 2011; 10(4):201–204.
9. Schuppe HC, Meinhardt A, Allam JP, Bergmann M, Weidner W, Haidl G. Chronic orchitis: a neglected cause of male infertility? *Andrologia*. 2008;40(2):84–91.
10. Lustig L, Lourtau L, Perez R, Doncel GF. Phenotypic characterization of lymphocytic cell infiltrates into the testes of rats undergoing autoimmune orchitis. *Int J Androl*. 1993;16(4):279–284.
11. Frungieri MB, et al. Number, distribution pattern, and identification of macrophages in the testes of infertile men. *Fertil Steril*. 2002;78(2):298–306.
12. Pavlovich CP, King P, Goldstein M, Schlegel PN. Evidence of a treatable endocrinopathy in infertile men. *J Urol*. 2001;165(3):837–841.
13. Skakkebaek NE, Rajpert-De Meyts E, Main KM. Testicular dysgenesis syndrome: an increasingly common developmental disorder with environmental aspects. *Hum Reprod*. 2001;16(5):972–978.
14. Gibson DA, Saunders PT. Estrogen dependent signaling in reproductive tissues — a role for estrogen receptors and estrogen related receptors. *Mol Cell Endocrinol*. 2012;348(2):361–372.
15. Li X, et al. Transgenic mice expressing p450 aromatase as a model for male infertility associated with chronic inflammation in the testis. *Endocrinology*. 2006;147(3):1271–1277.
16. Eddy EM, et al. Targeted disruption of the estrogen receptor gene in male mice causes alteration of spermatogenesis and infertility. *Endocrinology*. 1996;137(11):4796–4805.
17. Strauss L, et al. Increased exposure to estrogens disturbs maturation, steroidogenesis, and cholesterol homeostasis via estrogen receptor alpha in adult mouse Leydig cells. *Endocrinology*. 2009; 150(6):2865–2872.
18. Lin W, et al. Molecular mechanisms of bladder outlet obstruction in transgenic male mice overexpressing aromatase (Cyp19a1). *Am J Pathol*. 2011; 178(3):1233–1244.
19. Hardy MP, et al. Hormonal control of Leydig cell differentiation. *Ann N Y Acad Sci*. 1991;637:152–163.
20. Chang YF, Lee-Chang JS, Panneerdoss S, MacLean JA 2nd, Rao MK. Isolation of Sertoli, Leydig, and spermatogenic cells from the mouse testis. *Biotechniques*. 2011;51(5):341–342.
21. Mo R, Tony Zhu Y, Zhang Z, Rao SM, Zhu YJ. GAS6 is an estrogen-inducible gene in mammary epithelial cells. *Biochem Biophys Res Commun*. 2007; 353(1):189–194.
22. Fadok VA, Voelker DR, Campbell PA, Cohen JJ, Bratton DL, Henson PM. Exposure of phosphatidylserine on the surface of apoptotic lymphocytes triggers specific recognition and removal by macrophages. *J Immunol*. 1992;148(7):2207–2216.
23. Green DR, Reed JC. Mitochondria and apoptosis. *Science*. 1998;281(5381):1309–1312.
24. Daleke DL. Regulation of transbilayer plasma membrane phospholipid asymmetry. *J Lipid Res*. 2003;44(2):233–242.
25. Gong EY, Park E, Lee HJ, Lee K. Expression of Atp8b3 in murine testis and its characterization as a testis specific P-type ATPase. *Reproduction*. 2009; 137(2):345–351.
26. Santamarina-Fojo S, Remaley AT, Neufeld EB, Brewer HB Jr. Regulation and intracellular trafficking of the ABCA1 transporter. *J Lipid Res*. 2001;42(9):1339–1345.
27. Bitbol M, Fellmann P, Zachowski A, Devaux PF. Ion regulation of phosphatidylserine and phosphatidylethanolamine outside-inside translocation in human erythrocytes. *Biochim Biophys Acta*. 1987;904(2):268–282.
28. Stafford JH, Thorpe PE. Increased exposure of phosphatidylethanolamine on the surface of tumor vascular endothelium. *Neoplasia*. 2011;13(4):299–308.
29. Zhou Q, Zhao J, Stout JG, Luhm RA, Wiedmer T, Sims PJ. Molecular cloning of human plasma membrane phospholipid scramblase. A protein mediating transbilayer movement of plasma membrane phospholipids. *J Biol Chem*. 1997;272(29):18240–18244.
30. Wiedmer T, Zhou Q, Kwoh DY, Sims PJ. Identification of three new members of the phospho-lipid scramblase gene family. *Biochim Biophys Acta*. 2000;1467(1):244–453.
31. Williamson P, Bevers EM, Smeets EF, Comfurius P, Schlegel RA, Zwaal RF. Continuous analysis of the mechanism of activated transbilayer lipid movement in platelets. *Biochemistry*. 1995;34(33):10448–10455.
32. Fricker M, Neher JJ, Zhao JW, Thery C, Tolkovsky AM, Brown GC. MFG-E8 mediates primary phagocytosis of viable neurons during neuroinflammation. *J Neurosci*. 2012;32(8):2657–2666.
33. Segawa K, Suzuki J, Nagata S. Constitutive exposure of phosphatidylserine on viable cells. *Proc Natl Acad Sci U S A*. 2011;108(48):19246–19251.
34. Townsend EA, Thompson MA, Pabelick CM, Prakash YS. Rapid effects of estrogen on intracellular Ca^{2+} regulation in human airway smooth muscle. *Am J Physiol Lung Cell Mol Physiol*. 2010;298(4):L521–L530.
35. Miller VM, Duckles SP. Vascular actions of estrogens: functional implications. *Pharmacol Rev*. 2008;60(2):210–241.
36. Yanagita M, et al. Gas6 regulates mesangial cell proliferation through Axl in experimental glomerulonephritis. *Am J Pathol*. 2001;158(4):1423–1432.
37. Dormady SP, Zhang XM, Basch RS. Hematopoietic progenitor cells grow on 3T3 fibroblast monolayers that overexpress growth arrest-specific gene-6 (GAS6). *Proc Natl Acad Sci U S A*. 2000;97(22):12260–12265.
38. Huseby R. Leydig cell neoplasia. In: Payne AH, Hardy MP, Russell LD, eds. *The Leydig Cell*. Vienna, Austria: Cache River Press; 1996:555–572.
39. Qian YM, Sun XJ, Tong MH, Li XP, Richa J, Song WC. Targeted disruption of the mouse estrogen sulfotransferase gene reveals a role of estrogen metabolism in intracrine and paracrine estrogen regulation. *Endocrinology*. 2001;142(12):5342–5350.
40. Calippe B, et al. 17β-estradiol promotes TLR4-triggered proinflammatory mediator production through direct estrogen receptor alpha signaling in macrophages in vivo. *J Immunol*. 2010; 185(2):1169–1176.
41. Li X, et al. Multiple structural and functional abnormalities in the p450 aromatase expressing transgenic male mice are ameliorated by a p450 aromatase inhibitor. *Am J Pathol*. 2004;164(3):1039–1048.
42. Li X, et al. Altered structure and function of reproductive organs in transgenic male mice overexpressing human aromatase. *Endocrinology*. 2001; 142(6):2435–2442.
43. Huhtaniemi I, Nikula H, Rannikko S. Treatment of prostatic cancer with a gonadotropin-releasing hormone agonist analog: acute and long term effects on endocrine functions of testis tissue. *J Clin*

Endocrinol Metab. 1985;61(4):698–704.

44. Gooren L, et al. Sex steroids and pulsatile luteinizing hormone release in men. Studies in estrogen-treated agonadal subjects and eugonadal subjects treated with a novel nonsteroidal antiandrogen. *J Clin Endocrinol Metab*. 1987;64(4):763–770.

45. Finkelstein JS, O'Dea LS, Whitcomb RW, Crowley WF Jr. Sex steroid control of gonadotropin secretion in the human male. II. Effects of estradiol administration in normal and gonadotropin-releasing hormone-deficient men. *J Clin Endocrinol Metab*. 1991;73(3):621–628.

46. Sawin CT, Ryan RJ, Longcope C, Fisher LE. Effect of chronic administration of estrogen, androgen, or both on serum levels of gonadotropins in adult men. *J Clin Endocrinol Metab*. 1978;46(6):911–915.

47. Shang T, Zhang X, Wang T, Sun B, Deng T, Han D. Toll-like receptor-initiated testicular innate immune responses in mouse Leydig cells. *Endocrinology*. 2011;152(7):2827–2836.

48. Nagata K, et al. Identification of the product of growth arrest-specific gene 6 as a common ligand for Axl, Sky, and Mer receptor tyrosine kinases. *J Biol Chem*. 1996;271(47):30022–30027.

49. Whitacre CC, Reingold SC, O'Looney PA. A gender gap in autoimmunity. *Science*. 1999; 283(5406):1277–1278.

50. Straub RH. The complex role of estrogens in inflammation. *Endocr Rev*. 2007;28(5):521–574.

51. Serbina NV, Jia T, Hohl TM, Pamer EG. Monocyte-mediated defense against microbial pathogens. *Annu Rev Immunol*. 2008;26:421–452.

52. Taylor PR, Martinez-Pomares L, Stacey M, Lin HH, Brown GD, Gordon S. Macrophage receptors and immune recognition. *Annu Rev Immunol*. 2005;23:901–944.

53. Wang H, et al. Immunoexpression of Tyro 3 family receptors — Tyro 3, Axl, and Mer — and their ligand Gas6 in postnatal developing mouse testis. *J Histochem Cytochem*. 2005;53(11):1355–1364.

54. Lubahn DB, Moyer JS, Golding TS, Couse JF, Korach KS, Smithies O. Alteration of reproductive function but not prenatal sexual development after insertional disruption of the mouse estrogen receptor gene. *Proc Natl Acad Sci U S A*. 1993;90(23):11162–11166.

55. Okada H, Tajima A, Shichiri K, Tanaka A, Tanaka K, Inoue I. Genome-wide expression of azoospermia testes demonstrates a specific profile and implicates ART3 in genetic susceptibility. *PLoS Genet*. 2008;4(2):e26.

56. Johnsen SG. Testicular biopsy score count — a method for registration of spermatogenesis in human testes: normal values and results in 335 hypogonadal males. *Hormones*. 1970;1(1):2–25.